2011

DISTINCT ROLE OF NITRIC OXIDE AND PEROXYNITRITE IN MEDIATING OLIGODENDROCYTE TOXICITY IN CULTURE AND IN EXPERIMENTAL AUTOIMMUNE ENCEPHALOMYELITIS

S. Li
Uniformed Services University of the Health Science

A. C. Vana
Uniformed Services University of the Health Science

R. Ribeiro
Uniformed Services University of the Health Science

Y. Zhang
Uniformed Services University of the Health Sciences, yzhang@usuhs.mil

Neuroscience 184 (2011) 107–119

DISTINCT ROLE OF NITRIC OXIDE AND PEROXYNITRITE IN MEDIATING OLIGODENDROCYTE TOXICITY IN CULTURE AND IN EXPERIMENTAL AUTOIMMUNE ENCEPHALOMYELITIS

S. LI,[a] A. C. VANA,[a] R. RIBEIRO[b] AND Y. ZHANG[a,b]*

[a]*Department of Anatomy, Physiology and Genetics, Uniformed Services University of the Health Science, 4301 Jones Bridge Road, Bethesda, MD 20814, USA*

[b]*Program in Neuroscience, Uniformed Services University of the Health Science, 4301 Jones Bridge Road, Bethesda, MD 20814, USA*

Abstract—Nitric oxide has been implicated in the pathogenesis of multiple sclerosis. However, it is still unclear whether nitric oxide plays a protective role or is deleterious. We have previously shown that peroxynitrite, a reaction product of nitric oxide and superoxide, is toxic to mature oligodendrocytes (OLs). The toxicity is mediated by intracellular zinc release, phosphorylation of extracellular signal-regulated kinase 1/2 (ERK1/2), activation of 12-lipoxygenase (12-LOX) and the formation of reactive oxygen species (ROS). In this study, we found that the donors of nitric oxide, dipropylenetriamine NONOate (DPT NONOate) and diethylenetriamine NONOate (DETA NONOate), protected OLs from peroxynitrite or zinc-induced toxicity. The protective mechanisms appear to be attributable to their inhibition of peroxynitrite- or zinc-induced ERK1/2 phosphorylation and 12-LOX activation. In cultures of mature OLs exposed to lipopolysaccharide (LPS), induction of inducible nitric oxide synthase (iNOS) generated nitric oxide and rendered OLs resistant to peroxynitrite-induced toxicity. The protection was eliminated when 1400W, a specific inhibitor of iNOS, was co-applied with LPS. Using MOG35-55-induced experimental autoimmune encephalomyelitis (EAE), an animal model of multiple sclerosis, we found that nitrotyrosine immunoreactivity, an indicator of peroxynitrite formation, was increased in the spinal cord white matter, which correlated with the loss of mature OLs. Targeted gene deletion of the NADPH oxidase component gp91phox reduced clinical scores, the formation of nitrotyrosine and the loss of mature OLs. These results suggest that blocking the formation specifically of peroxynitrite, rather than nitric oxide, may be a protective strategy against oxidative stress induced toxicity to OLs. Published by Elsevier Ltd on behalf of IBRO.

Key words: nitric oxide, peroxynitrite, NADPH oxidase, zinc, oligodendrocytes, experimental autoimmune encephalomyelitis.

Upregulation of inducible nitric oxide synthase (iNOS) and the generation of nitric oxide (NO) in reactive microglia/macrophages is a common feature in multiple sclerosis (MS) (Smith and Lassmann, 2002; Hill et al., 2004; Saha and Pahan, 2006). Although there is an increased understanding as to the physiological and pathological properties of nitric oxide in health and disease, the role of NO in the pathogenesis of MS is still not well defined (Encinas et al., 2005; Willenborg et al., 2007). The sources of NO, the amount and sites of NO production, and the molecules NO reacts with might contribute to the great variability of the disease promoting or suppressing effects in MS.

NO is synthesized from the amino acid L-arginine by NO synthase (NOS). There are three major isoforms of NOS: neuronal NOS (nNOS), endothelial NOS (eNOS) and inducible NOS (iNOS). nNOS and eNOS are constitutively expressed and require calcium and calmodulin for activation, whereas iNOS is largely calcium independent and induced in inflammatory conditions (Knowles and Moncada, 1994). Although nNOS and eNOS have been shown to be elevated in experimental autoimmune encephalomyelitis (EAE), one of the commonly used animal models of MS (Wu and Tsirka, 2009; Yao et al., 2010), iNOS induction in reactive microglia/macrophages and astrocytes is believed to be the predominant source of NO (Broholm et al., 2004; Sun et al., 2010). It is known that NO is neither a potent oxidant nor a strong reductant (Calabrese et al., 2009), but it can rapidly react with superoxide to produce the powerful oxidant peroxynitrite (Beckman et al., 1990; Pacher et al., 2007). Uric acid, a competitive inhibitor of tyrosine nitration by peroxynitrite (Robinson et al., 2004), and FeTPPS, a decomposition catalyst of peroxynitrite (Misko et al., 1998), have been shown to be protective in the EAE animal models of MS (Hooper et al., 1998; Cross et al., 2000; Hooper et al., 2000; Bolton et al., 2008). These results are consistent with the findings that patients with MS and hyperuricemia are mutually exclusive (Spitsin et al., 2001; Scott et al., 2002). Although several studies suggest that inhibitors of iNOS ameliorate EAE (Brenner et al., 1997; Hooper et al., 1997), mice with targeted gene deletion of iNOS (iNOS−/−) are found to have an in-

*Correspondence to: Y. Zhang, Department of Anatomy, Physiology and Genetics, Uniformed Services University of the Health Sciences, 4301 Jones Bridge Road, Bethesda, MD 20814, USA. Tel: +1-301-295-3212; fax: +1-301-295-3566.
E-mail address: yzhang@usuhs.mil (Y. Zhang).

Abbreviations: BDM, basal chemically-defined medium; BSA, bovine serum albumin; CNTF, ciliary neurotrophic factor; DCF, 2′, 7′-dichlorohydrofluorescein diacetate; DEA NONOate, diethylamine NONOate; DETA NONOate, diethylenetriamine NONOate; DPTA NONOate, dipropylenetriamine NONOate; DHR, dihydrorhodamine 123; EAE, experimental autoimmune encephalomyelitis; EBSS, Earle's balanced salt solution; eNOS, endothelial nitric oxide synthase; ERK1/2, extracellular signal-regulated kinase 1/2; HBSS, Hank's balanced salt solution; IHC, immunohistochemistry; iNOS, inducible nitric oxide synthase; LOX, lipoxygenase; LPS, lipopolysaccharide; MOG 35–55, myelin oligodendrocyte glycoprotein peptide 35–55; MS, multiple sclerosis; nNOS, neuronal nitric oxide synthase; NO, nitric oxide; OL, oligodendrocyte; ROS, reactive oxygen species; sGC, soluble guanylate cyclase; TBST, Tris-buffered saline containing 0.1% Tween 20; 12-HETE, 12-hydroxyeicosatetraenoic acid.

0306-4522/11 $ - see front matter. Published by Elsevier Ltd on behalf of IBRO.
doi:10.1016/j.neuroscience.2011.04.007

creased disease severity (Fenyk-Melody et al., 1998; Sahrbacher et al., 1998). These results suggest that the interaction and balance between nitric oxide, superoxide and peroxynitrite might be critical in determining whether the combined action of these reactive nitrogen and oxygen species is protective or deleterious.

We have previously shown that peroxynitrite toxicity to mature oligodendrocytes (OLs) is mediated by intracellular zinc release, activation of extracellular signal-regulated kinase 1/2 (ERK1/2), 12-lipoxygenase (12-LOX) and the formation of reactive oxygen species (ROS) (Zhang et al., 2006). We also found that 12-LOX activation contributes to OL toxicity induced by glutathione depletion (Wang et al., 2004). Similar to 5-LOX (Coffey et al., 2000, 2002), the activity of 12-LOX is also regulated by the intracellular redox status (Shornick and Holtzman, 1993), and can be inhibited by nitric oxide (Nakatsuka and Osawa, 1994; Fujimoto et al., 1998; Coffey et al., 2001). Therefore, it is likely that nitric oxide may attenuate peroxynitrite-induced toxicity to OLs via inhibition of 12-LOX. In this study, we found that both exogenously applied and endogenously generated nitric oxide is protective against peroxynitrite toxicity to OLs. The protective mechanisms appeared to be attributable to the direct interaction of nitric oxide with 12-LOX and the signaling molecules upstream of 12-LOX activation. Using myelin oligodendrocyte glycoprotein (MOG)-induced EAE mouse model, we found that mice with targeted gene deletion of gp91phox (gp91phox−/−), a catalytic component of NADPH oxidase (Babior et al., 2002), are resistant to EAE. These results suggest that although peroxynitrite, the reaction product of nitric oxide and superoxide, is toxic to OLs, nitric oxide per se can serve as a potent antioxidant and an anti-inflammatory agent.

EXPERIMENTAL PROCEDURES

Materials

SIN-1, peroxynitrite, diethylamine NONOate (DEA NONOate), dipropylenetriamine NONOate (DPT NONOate) and diethylenetriamine NONOate (DETA NONOate) were obtained from Cayman Chemical Co. (Ann Arbor, MI, USA). FluoZin-3, RhodZin-3, dihydrorhodamine 123 (DHR) and 2′,7′-dichlorohydrofluorescein diacetate (DCF) were purchased from Molecular Probes, Inc. (Eugene, OR, USA). All the culture materials were purchased from Gibco Life Technologies (Grand Island, NY, USA). Platelet-derived growth factor (PDGF), basic fibroblast growth factor (bFGF), and ciliary neurotrophic factor (CNTF) were purchased from Peprotech (Princeton, NJ, USA). All other reagents were obtained from Sigma (St. Louis, MO, USA).

Oligodendrocyte culture

Primary cultures of OLs were prepared by shaking off the progenitor cells from mixed glial cell cultures as previously described (Wang et al., 2004; Zhang et al., 2006). Briefly, mixed primary glial cultures were prepared from 3 day-old Sprague–Dawley rats by dissociation of the brains after they were dissected from the pups. Cultures were maintained in Dulbecco's modified Eagle's medium (DMEM) containing 20% heat-inactivated fetal bovine serum and 1% penicillin/streptomycin in poly-lysine coated 75 cm^2 flasks incubated in 95% air/5% CO_2, at 37 °C. The media were changed three times per week until the cells were confluent (7–10 days). The flasks were then shaken for 1 h on an orbital shaker (200 rpm) at 37 °C to remove microglia. They were then changed to new media and shaken overnight. The OL progenitor cells were detached from the astrocyte layer and were resuspended and seeded onto poly-ornithine coated plates [96-well (2×10^5 cells/plate), 24-well (4×10^5 cells/plate)] in a basal chemically-defined medium (BDM) [DMEM with 1 mg/ml bovine serum albumin (BSA), 50 μg/ml apo-transferrin, 5 μg/ml insulin, 30 nM sodium selenite, 10 nM biotin, 10 nM hydrocortisone] plus 10 ng/ml of both PDGF and bFGF. The cells were maintained in BDM and the medium was half-changed three times per week. For culturing mature OLs, at day 7 OLs were changed to BDM plus 3,3′,5-triodo-L-thyronine (T_3) (15 nM) and CNTF (10 ng/ml) and were half-changed three times per week for 2 weeks. At this stage, more than 95% of the cells were MBP positive (Baud et al., 2004; Wang et al., 2004) and were used for the experiments. The contamination of astrocytes and microglia was 1–2%, each.

Toxicity assay

The survival of cells after various treatments in 96-well plates were evaluated by visual inspection using phase contrast microscopy and quantified by using Alamar Blue (Trek Diagnostic Systems, Inc., Westlake, OH, USA), a viability assay that was previously described and validated by cell counting using Trypan Blue exclusion (Back et al., 1999). In all experiments, the culture plates were first washed twice with Hank's Balanced Salt Solution (HBSS) containing 0.1% BSA and then placed in Earle's Balanced Salt Solution (EBSS, which is composed of 116 mM NaCl, 5.4 mM KCl, 1.8 mM $CaCl_2$, 0.8 mM $MgSO_4$, 26 mM $NaHCO_3$, 1 mM NaH_2PO_4 and 5.5 mM D-glucose). OLs were treated with SIN-1, a peroxynitrite donor, peroxynitrite or zinc chloride ($ZnCl_2$) for 2 h, washed twice with HBSS containing 0.1% BSA, and then placed in BDM with T3 and CNTF. Unless specifically described, donors of nitric oxide were applied 15 min before, during and after the cells were exposed to SIN-1, peroxynitrite or $ZnCl_2$. After the cells were incubated for 20–24 h, the culture medium was replaced with EBSS plus a 1:100 dilution of Alamar Blue. After a 2 h exposure, the fluorescence of the Alamar Blue solution in each well in the plates was read at room temperature in a fluorescent plate reader (SpectraMax Germini XS, GMI Inc., MN, USA) with excitation wavelength at 530 nm and emission wavelength at 590 nm. The data from Alamar Blue assays matched the results from visual inspection.

Measurement of intracellular cGMP

Intracellular cGMP content was assayed by enzyme-linked immunoassay (Amersham, Piscataway, NJ, USA). Cultures were washed twice and medium was replaced by EBSS in the absence or presence of DPT-NONOate, SIN-1, and their combination. The nonspecific phosphodiesterase inhibitor, 3-isobutyl-1-methylxanthine (IBMX) at 100 μM was present in all conditions. After 30 min treatment with DPT-NONOate and SIN-1, medium was replaced with 200 μl of releasing reagent provided in the kit. The plates were agitated for 20 min at room temperature, and 20 μl of acetylation reagent was added. After 5 min, 50 μl samples were taken for assaying the intracellular content of cGMP.

Fluorescence imaging of intracellular liberation of zinc

Changes in intracellular free zinc concentration in OLs were monitored with a high affinity, zinc selective indicator, FluoZin-3 (Gee et al., 2002). OLs in 24-well plates were loaded with FluoZin-3 (1 μM) for 30 min, washed with HBSS containing 0.1% BSA, and then treated with SIN-1 (1 mM) in the absence or presence of DPT-NONOate (30 μM) for 60 min. The fluorescence imaging of

intracellular zinc was monitored immediately using digital fluorescence microscopy (Nikon TE-2000) with a 20× objective (excitation at 485 nm, emission at 530 nm). For all images, the microscope settings, such as brightness, contrast and exposure time, were held constant to compare the relative intensity of intracellular zinc fluorescence across all treatment conditions.

For quantitative analysis, OLs in 96-well plates were loaded with FluoZin-3 (2 μM) or RhodZin-3 (2 μM) for 30 min, washed twice, and then treated with SIN-1 (1 mM) in the absence or presence of DPT-NONOate (30 μM) for 60 min. The fluorescence intensity, an indicator of intracellular zinc liberation, in each well was read at excitation and emission pairs, 485 nm/530 nm and 550 nm/575 nm, for FluoZin-3 and RhodZin-3, respectively.

Measurement of 12-LOX activity

12-LOX activity was measured by quantifying the major metabolic product of 12-LOX, 12-hydroxyeicosatetraenoic acid (12-HETE), by ELISA (Assay Designs Inc., Ann Arbor, MI, USA). OLs were treated with SIN-1 with/without DPT-NONOate for 60 min. After the cultures were washed twice with HBSS containing 0.1% BSA, arachidonic acid (20 μM) in EBSS was added to the culture which was then incubated for 30 min. The medium was then collected, extracted and assayed for 12-HETE according to the manufacturer's protocol. The concentration of 12-HETE in each sample was normalized to the sample's protein concentration.

Measurement of intracellular ROS generation

Intracellular free radical generation was evaluated with DHR and DCF (Molecular Probes, Eugene, OR, USA) as we previously described (Wang et al., 2004; Zhang et al., 2006). Briefly, after the cells in 24-well and 96-well plates were treated with SIN-1 with/without DPT-NONOate for 60 min, they were loaded with DHR (20 μM) or DCF (20 μM) for 30 min in EBSS (95% air/5% CO_2, 37 °C). After the loading solution was removed, the cells in the wells were washed and incubated in EBSS. For fluorescence imaging of the oxidized DHR, cells in 24-well plates were visualized using a digital fluorescent microscope (Nikon TE-2000) with a 20× objective. For all images, the microscope settings, such as brightness, contrast and exposure time, were held constant to compare the relative intensity of oxidized rhodamine across all treatment conditions. The DCF fluorescence of the cells in each well was measured and recorded in the fluorescent plate-reader described above (with excitation wavelength at 480 nm and emission wavelength at 530 nm and temperature at 37 °C).

Western blot analyses

At various time points after SIN-1 or zinc treatment, OLs were placed on ice. Following medium aspiration, cells were washed once with ice-cold phosphate-buffered saline, and lysed with lysis buffer containing 20 mM Tris, pH 7.5, 150 mM NaCl, 1 mM EDTA, 1 mM EGTA, 1% Triton X-100, 2.5 mM sodium pyrophosphate, 1 mM glycerolphosphate, 1 mM Na_3VO_4, and 1 mM phenylmethylsulfonyl fluoride. An aliquot of cell lysate was removed for later protein determination. Cell lysate was mixed with Laemmli buffer, boiled for 5 min, and stored at −20 °C. Equal amounts of protein were separated by 4–12% SDS-PAGE and electrotransferred to a polyvinylidene difluoride (PVDF) membrane. Membranes were blocked with 5% nonfat milk in Tris-buffered saline containing 0.1% Tween 20 (TBST) for 1 h and then incubated overnight at 4 °C with the primary antibodies for phosphorylated ERK1/2, total ERK1/2 (Cell Signaling, Beverly, MA, USA) and iNOS (BD Biosciences Pharmingen) diluted at 1:1000 in TBST containing 5% BSA. After washing four times with TBST, the membrane was incubated for 1 h at room temperature with a horseradish peroxidase-conjugated anti-rabbit secondary antibody (Santa Cruz Biotechnology, Santa Cruz, CA, USA) diluted at 1:4000. The membranes were washed again as above and visualized by enhanced chemiluminescence (ECL) according to the manufacturer's protocol (PerkinElmer Life Sciences).

For protein tyrosine nitration assay in the cell-free system, BSA (0.5 mg/ml) in EBSS with or without DPT-NONOate, DETA-NONOate and FeTPPS was exposed to SIN-1 for 1 h, and then 4× Laemmli buffer was added. After the samples were heated for 5 min, 2 μg protein per lane was subjected to SDS-PAGE analysis, followed by transfer to PVDF membrane and reacted with a mouse anti-nitrotyrosine monoclonal antibody (Upstate Biotechnology, Lake Placid, NY, USA). Protein was visualized with a horseradish peroxidase-conjugated sheep anti-mouse secondary antibody followed by detection with ECL.

Mice

Female 7–9-week-old gp91phox knockout mice (gp91phox−/−) on a C57BL/6J background and age matched C57BL/6J control mice were purchased from The Jackson Laboratory (Bar Harbor, ME, USA). Animal care and experimental procedures were carried out in accordance with the NIH guideline and approved by the Uniformed Services University Animal Care and Use Committee.

Induction and clinical evaluation of EAE

EAE in gp91phox−/− and C57BL/6J control mice was induced by s.c. injection of 200 μg MOG peptide 35–55 in Complete Freunds Adjuvant (CFA, DIFCO) with 500 μg *Mycobacterium tuberculosis* (DIFCO). Immediately following MOG peptide injection, and 24 h later, mice were administered with 200 ng pertusis toxin (List Biological Laboratories, Campbell, CA, USA) i.p. At 1 week after induction, EAE mice received a booster of 200 μg of MOG in incomplete Freunds Adjuvant without *Mycobacterium tuberculosis*. For gp91phox−/− and control mice without EAE induction, animals underwent the same procedures, except no MOG peptide was injected. Each group had eight animals. Animals were monitored blind by two independent observers from day 10 onwards and neurological signs were assessed as follows: 0, normal mouse; 1, piloerection, tail weakness; 2, tail paralysis; 3, tail paralysis plus hind limb weakness/paralysis; 4, tail, hind and fore limb paralysis; 5, moribund/death, using increments of 0.5 points for intermediate clinical findings. The onset of EAE was defined as the first day an animal showed a clinical score ≥0.5.

Immunohistochemistry (IHC)

Animals were euthanized using a combination of ketamine and xylazine solution (90 mg ketamine/10 mg xylazine per ml, i.p.), then intracardially perfused with ice cold 1 M phosphate buffer followed by 4% paraformaldehyde (Sigma, St. Louis, MO, USA) in 1 M phosphate buffer. Spinal cords were dissected out prior to post-fixation in 4% paraformaldehyde at 4 °C overnight. Tissue was then cryoprotected in 30% sucrose (Sigma) in 1 M phosphate buffer at 4 °C overnight. After being cryoprotected the tissue was embedded in Tissue Tek OCT (Sakura, Torrance, CA, USA) and stored at −80 °C until utilization. Transverse sections of lumbar spinal cords were cut at 14 μm with a cryostat (Leica model CM1900, Bannockburn, IL, USA) and mounted onto Superfrost plus slides (Fisher, Pittsburgh, PA, USA) for immunohistochemical analysis. For identification of activated microglia/macrophages, we used F4/80 antibody (eBioscience, San Diego, CA, USA). Nitrotyrosine reactivity in spinal cord white matter was examined using an anti-nitrotyrosine polyclonal antibody. Mature OLs were stained with antibody for CC1 (Calbiochem, San Diego, CA, USA).

Statistics

Cell densities in lumbar spinal cord white matter were manually counted with areas measured using Spot 2 software. Statistical

significance *in vitro* and *in vivo* assays was assessed using ANOVA with the Tukey–Kramer post hoc multiple comparison test. Statistical analysis was performed using the Instat program from GraphPad Software (San Diego, CA, USA). Experiments were performed with triplicate samples, and the data are expressed as mean±SD. All experiments were repeated at least three times.

RESULTS

Effects of nitric oxide donors on peroxynitrite toxicity to mature OLs

Although nitric oxide is able to react with superoxide to form the powerful oxidant, peroxynitrite, nitric oxide per se can function as an antioxidant (Thomas et al., 2008; Sun et al., 2010). It has been shown previously that several donors of nitric oxide prevent cysteine depletion induced toxicity to OLs (Rosenberg et al., 1999). DPT-NONOate and DETA-NONOate, with half-lives of 3 h and 20 h (Mooradian et al., 1995), respectively, had significant protective effects, whereas DEA-NONOate, with a short half-life of only 2.1 min (Maragos et al., 1991), did not exert any protection. The failure of DEA-NONOate to protect OLs from injury is likely due to the fact that there is no continuous release or sustained effective concentrations of nitric oxide available to antagonize the late oxidative stress triggered by glutathione depletion. Using the same nitric oxide donors, we tested the role of nitric oxide on SIN-1, a peroxynitrite generator, as well as peroxynitrite induced toxicity to mature OLs. As shown in Fig. 1, DPT-NONOate and DETA-NONOate protected against SIN-1 or peroxynitrite induced toxicity to mature OLs in a concentration-dependent manner. DPT-NONOate at 30 μM near fully attenuated peroxynitrite toxicity. The maximal protection of DETA-NONOate was found at 100 μM. However, DEA-NONOate either at 30 μM or 100 μM did not have any protective effect.

To exclude the possibility that nitric oxide may react with peroxynitrite directly, we examined whether protein nitration evoked by SIN-1 can be altered by the presence of nitric oxide donors. Consistent with our previous findings (Zhang and Rosenberg, 2002), SIN-1 at 1 mM caused a strong tyrosine nitration of BSA in a cell-free system. The nitration was completely blocked by FeTPPS (10 μM), a decomposition catalyst of peroxynitrite, but not by DPT-NONOate (30 μM and 100 μM) or DETA-NONOate (100 μM). Protein nitration was not found when the BSA solution was treated by DPT-NONOate, DETA-NONOate and FeTPPS themselves (Fig. 2A).

It is known that nitric oxide can activate soluble guanylyl cyclase (sGC), resulting in the production of cGMP (Murad et al., 1993). If the generation of nitric oxide by nitric oxide donors is affected by the presence of SIN-1, the production of cGMP in OLs is likely to be altered. Exposure of OLs with DPT-NONOate (30 μM) or SIN-1 (1 mM) for 30 min caused a four-fold increase in the production of cGMP. The combination of DPT-NONOate and SIN-1 did not have any additive or suppressive effect (Fig. 2B). This result suggests that the effective nitric oxide concentration generated by DPT-NONOate is not reduced by the presence of SIN-1.

To further exclude the possibility that a direct interaction of nitric oxide donors with SIN-1 may reduce the availability of peroxynitrite, donors of nitric oxide were added at various times after initiation of OLs exposure to peroxynitrite. Because the half life of peroxynitrite is only a few seconds at physiological pH (Szabo et al., 2007), delayed addition of nitric oxide is expected to prevent the direct interaction of nitric oxide with peroxynitrite. Similar to the results obtained by co-administration of donors of nitric oxide and peroxynitrite, delayed addition of DPT-NONOate (30 μM) and DETA-NONOate (100 μM) at 30 min following peroxynitrite exposure significantly protected OLs from toxicity (Fig. 2C). However, no protection was observed when nitric oxide donors were added 60 min after peroxynitrite treatment (Fig. 2C). These results suggest that the protective effects of various donors of nitric oxide not only depend on the amount and the duration of nitric oxide released, but also depend on the direct interaction of nitric oxide with the signaling molecules activated at the selective time window following oxidative stress.

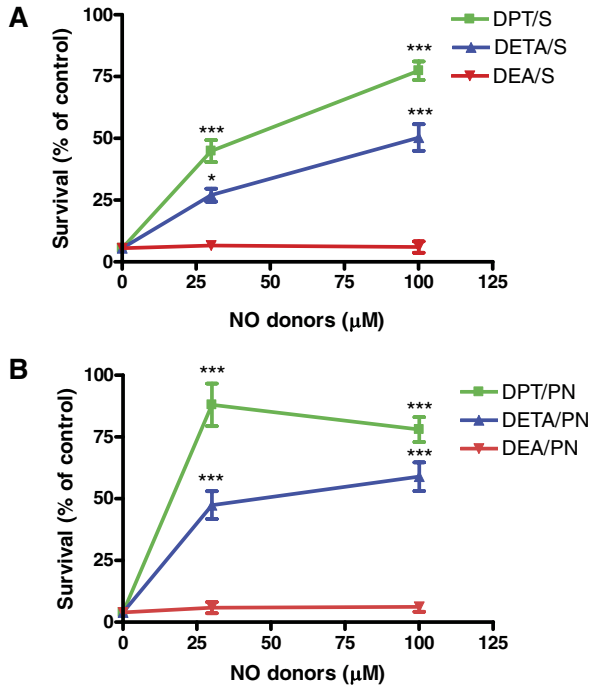

Fig. 1. Effects of nitric oxide donors on peroxynitrite toxicity to mature OLs. Mature OLs were exposed to SIN-1 (A) or peroxynitrite (B) alone or with 30 μM and 100 μM DEA-NONOate (DEA), DPTA-NONOate (DPT), or DETA-NONOate (DETA) for 2 h, and at an additional 20–24 h cell death was determined by Alamar Blue reduction. SIN-1 at 1 mM or peroxynitrite (PN) at 300 μM caused near total OL cell death. DEA, with a half-life in aqueous solution of 2 min, did not have a protective effect, whereas DPT and DETA, with half-lives in aqueous solutions of 3 and 20 h, respectively, were protective. * $P<0.05$ and *** $P<0.001$ were obtained when the DPT- or the DETA- treated groups were compared with the SIN-1 (S) or PN group alone. Data shown in (A) and (B) are pooled from six different experiments. For interpretation of the references to color in this figure legend, the reader is referred to the Web version of this article.

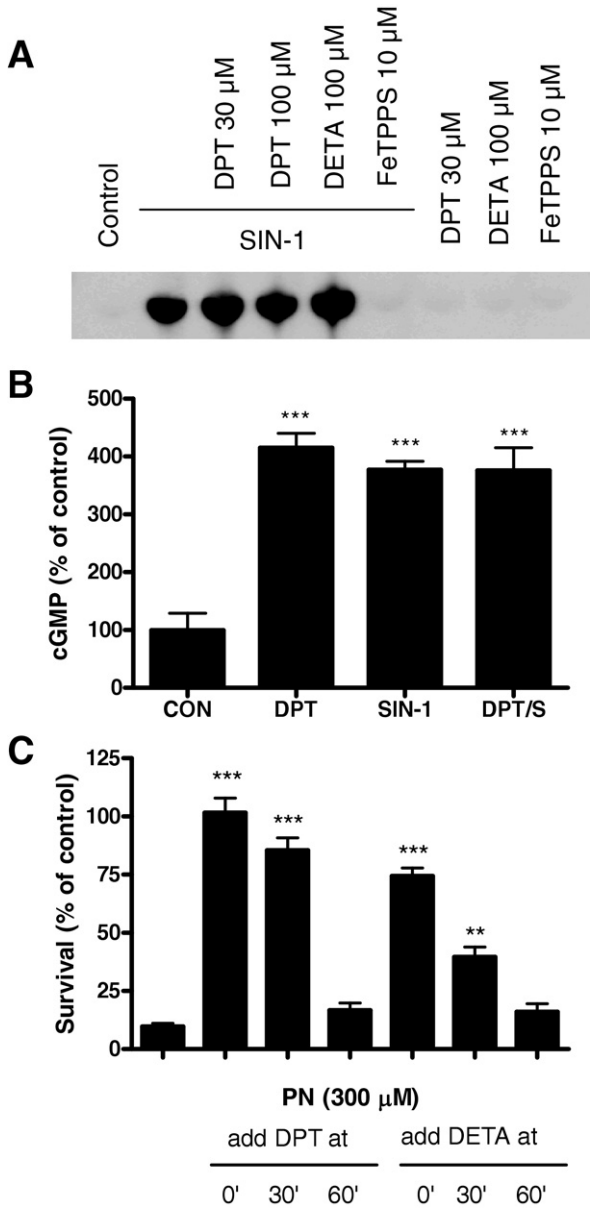

Fig. 2. The protective effect of nitric oxide donors on peroxynitrite toxicity is not due to the direct interaction between nitric oxide and peroxynitrite. (A) DPT and DETA did not attenuate protein nitration evoked by SIN-1. BSA (0.5 mg/ml) in EBSS was exposed to SIN-1 (1 mM) for 1 h either alone or in the presence of DPT, DETA or FeTPPS. BSA nitration caused by SIN-1 was not affected by the presence of nitric oxide donors, but completely blocked by FeTPPS, a decomposition catalyst of peroxynitrite. A representative experiment of three that were performed is shown. (B) DPT and SIN-1 enhanced cGMP accumulation in OLs. OLs were treated with DPT (30 μM), SIN-1 (1 mM), DPT plus SIN-1 for 30 min, and then lysed for measurement of the intracellular cGMP content. DPT and SIN-1 both caused a 4-fold increase of cGMP. The combination of DPT and SIN-1 had no additional effect. *** $P<0.001$ was obtained when the DPT, SIN-1, and DPT plus SIN-1 (DPT/S) treated groups were compared with the control group. Data shown are pooled from three different experiments. (C) Delayed treatment of DPT or DETA on OL toxicity induced by peroxynitrite. Cultures that were exposed to 300 μM peroxynitrite (PN) were given DPT (30 μM) or DETA (100 μM) at various times (0, 30 and 60 min) following PN exposure and the toxicity was assessed at 24 h. Simultaneous administration of DPT and DETA with PN resulted in 98±11% and 75±6% protection, respectively. Delayed addition of DPT or DETA at 30 min following PN exposure also protected against PN toxicity. Cell survival in the presence of DPT and DETA was 80±6% and 35±11%, respectively. Protective effects were not observed when the nitric oxide donors were given at 60 min following PN exposure. ** $P<0.01$ and *** $P<0.001$ were obtained when the DPT- and the DETA-treated groups ($n=3$) were compared with the PN group alone ($n=3$).

Nitric oxide blocked SIN-1 induced 12-LOX activation and ROS generation

We have found that peroxynitrite toxicity to mature OLs is mediated by 12-LOX activation and the subsequent generation of ROS (Zhang et al., 2006). To test whether the protective effects of nitric oxide are due to its inhibition of 12-LOX activity and blockade of ROS generation, mature OLs were treated with SIN-1 for 60 min, and the activity of 12-LOX and the generation of ROS were assessed. Using ELISA, we examined the activity of 12-LOX by measuring the 12-LOX metabolic end product, 12-HETE. We found that exposure of OLs to SIN-1 for 60 min induced a significant increase of 12-LOX activity (Fig. 3A). The level of 12-LOX activity in SIN-1 (1 mM, 1 h) treated OLs was 150±8% (mean±SD, $n=3$) of control. DPT-NONOate at 30 μM completely blocked SIN-1 induced activation of 12-LOX (Fig. 3A). To test the effect of nitric oxide on ROS generation, mature OLs were treated with SIN-1 for 60 min, and then exposed to DHR or DCF for 30 min. SIN-1 at 1 mM caused a dramatic increase of ROS generation, as indicated by the elevation of DHR fluorescence. DPT-NONOate (30 μM), did not cause ROS generation, but completely blocked the generation of ROS induced by SIN-1 (Fig. 3B). The same result was also found when the ROS generation was quantified using DCF as an indicator. SIN-1 caused a time-dependent increase of ROS generation, which was almost completely blocked by DPT-NONOate (Fig. 3C).

DPT-NONOate reduced SIN-1 induced intracellular zinc release and ERK1/2 phosphorylation

As we have shown previously, 12-LOX activation in mature OLs induced by SIN-1 occurs downstream of intracellular zinc release and ERK1/2 phosphorylation (Zhang et al., 2006). Therefore, it is possible that donors of nitric oxide may directly interact with these signaling molecules. Mature OLs were treated with SIN-1 in the absence or presence of DPT-NONOate (30 μM) for various times (0, 15, 30, 60, 90 and 120 min), and then lysed for determining the levels of the phosphorylated and the total ERK1/2 by western blot analysis. SIN-1 (1 mM) induced phosphorylation of ERK1/2 appeared at 60 min, and further increased at 90 min and 120 min. The increased ERK1/2 phosphorylation was significantly attenuated by DPT-NONOate (30 μM) (Fig. 4A). Using densitometric analysis, we found that DPT-NONOate resulted in a 40–50% reduction in the ratio of the phosphorylated and the total ERK1/2 at 60, 90 and 120 min after SIN-1 treatment (Fig. 4B).

Similar to other oxidizing agents (Aizenman et al., 2000), SIN-1 was also found to liberate zinc from intracel-

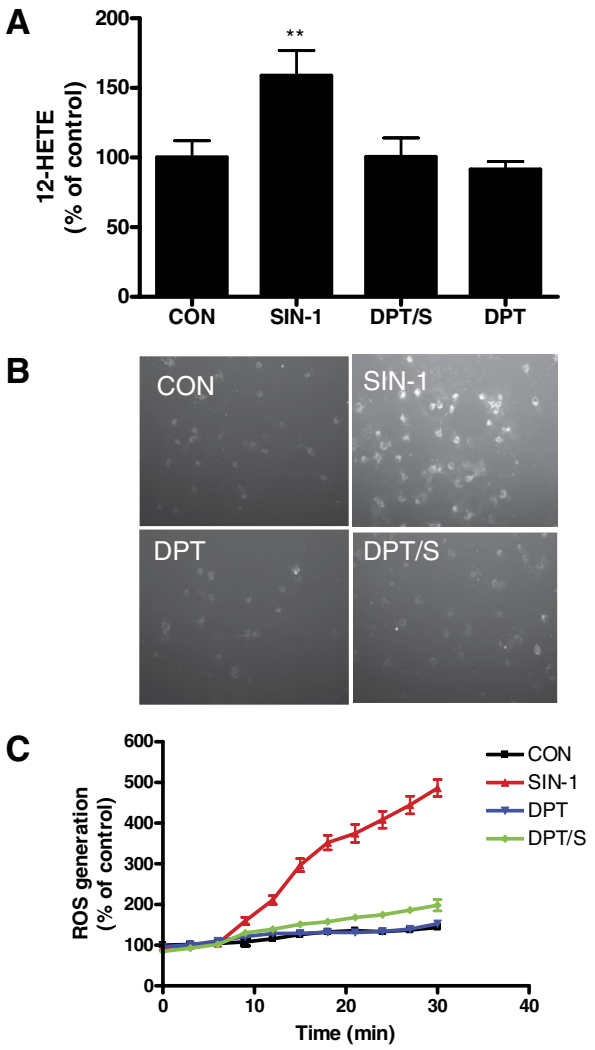

Fig. 3. DPT-NONOate attenuated 12-LOX activation and ROS generation in OLs induced by SIN-1. (A) DPT blocked activation of 12-LOX induced by SIN-1. Exposure of SIN-1 (1 mM) to OLs for 1 h induced a significant increase of 12-LOX activity. DPT (30 μM) completely blocked the activation of 12-LOX induced by SIN-1. ** $P<0.01$ was obtained when the SIN-1 alone group was compared with the other groups. The data are pooled from four different experiments. (B) SIN-1 induced ROS generation was blocked by DPT. OLs were treated with SIN-1 for 60 min in the absence or presence of DPT (30 μM) and then exposed to DHR for 30 min. SIN-1 caused an increase of ROS generation, which was attenuated by DPT. A representative experiment of three that were performed is shown. (C) OLs were treated with SIN-1 for 60 min in the absence or presence of DPT (30 μM) and then exposed to DCF for 30 min. SIN-1 caused a time-dependent increase of ROS generation, which was almost completely blocked by DPT. The data are pooled from three different experiments. For interpretation of the references to color in this figure legend, the reader is referred to the Web version of this article.

lular stores and zinc containing proteins, such as metallothionins (Zhang et al., 2004; Zhang et al., 2006). It is known that nitric oxide can cause intracellular zinc release by nitrosation of the zinc binding proteins (Maret, 2006). These results lead us to hypothesize that nitric oxide and peroxynitrite may have an additive or a synergistic effect in causing intracellular zinc liberation. Surprisingly, DPT-NONOate (30 μM) itself did not cause zinc release. It also had no effect on zinc liberation induced by SIN-1 (Fig. 4C). Using a quantitative analysis, we found that treatment with SIN-1 for 1 h caused a three-fold increase in the intracellular fluorescence intensity of FluoZin-3, which was not altered by the presence of DPT-NONOate. The same result was also found when RhodZin-3, another novel and highly selective zinc indicator (Sensi et al., 2003), was used (data not shown).

Donors of nitric oxide attenuated ERK1/2 phosphorylation, ROS generation and OL toxicity induced by exogenous zinc

To further determine whether the protective effects of nitric oxide on peroxynitrite induced toxicity to mature OLs are due to their interference with the cell death pathways triggered by zinc, rather than blocking zinc release, we tested the effects of nitric oxide donors on OL toxicity induced by exogenous zinc. Similar to the protective effects on SIN-1 or peroxynitrite induced toxicity, DPT-NONOate and DETA-NONOate showed significant protection against OL toxicity induced by $ZnCl_2$ (300 μM) (Fig. 5A). On the other hand, DEA-NONOate had no effect. As suggested previously, the different efficacy of these donors of nitric oxide might be due to their different half-lives and the effective concentrations of nitric oxide interacting with molecules implicated in cell death. Consistent with the protective mechanisms against peroxynitrite toxicity, donors of nitric oxide also attenuated zinc-induced ERK1/2 phosphorylation (Fig. 5B, C) and ROS generation (Fig. 5D).

Mature OLs in culture preconditioned with LPS are resistant to SIN-1 induced toxicity

It has been demonstrated that the expression of iNOS in cultures of OLs is not derived from OLs, but from the contamination of microglia and astrocytes (Hewett et al., 1999). Our culture preparation of OLs typically contains more than 95% OLs, 1–2% microglia and 1–2% astrocytes (Wang et al., 2004; Zhang et al., 2006). Because of the presence of only small numbers of microglia and astrocytes, treatment of these cultures with LPS can result in iNOS induction and NO production without damaging OLs. We speculated that pretreatment of cultures with LPS (5 μg/ml) for 24 h could enable OLs resistant to SIN-1 or peroxynitrite induced toxicity. Indeed, we found that without LPS preconditioning, cell viability in the presence of SIN-1 (0.5 mM) was 40±7%, and the cell viability increased to 80±10% when the preconditioned cultures were exposed to SIN-1 (Fig. 6A). To determine whether the protective effects of LPS preconditioning is due to the generation of nitric oxide, rather than other factors released from reactive microglia, cultures of mature OLs were also treated with 1400W, a selective inhibitor of iNOS, in the presence of LPS. As shown in Fig. 6A, the protection afforded by LPS preconditioning on SIN-1 induced toxicity was attenuated by 1400W (10 μM). 1400W, either used alone or together with LPS, did not affect the viability of OLs in the absence of SIN-1

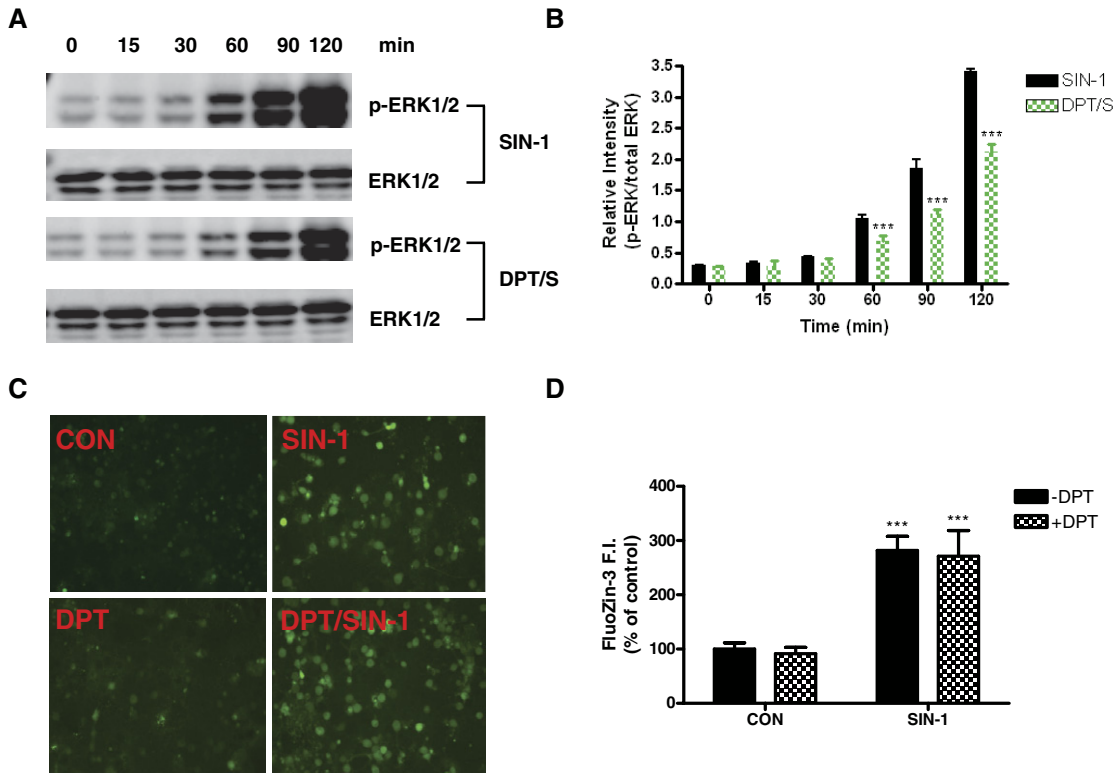

Fig. 4. DPT-NONOate attenuated SIN-1 induced ERK1/2 phosphorylation and zinc release in OLs. (A) DPT attenuated ERK1/2 phosphorylation induced by SIN-1. Exposure of SIN-1 (1 mM) to OLs induced time-dependent increase of ERK1/2 phosphorylation. DPT (30 μM) significantly reduced ERK1/2 phosphorylation. p-ERK refers to the phosphorylated ERK. A representative experiment of four that were performed is shown. (B) The relative intensity of the p-ERK/total ERK at various times following SIN-1 treatment was measured using densitometry. *** $P<0.001$ was obtained when the DPT plus SIN-1 group ($n=4$) was compared to the SIN-1 alone group ($n=4$) at the corresponding time points. (C) DPT attenuated the increase of FluoZin-3 fluorescence induced by SIN-1. OLs were treated with SIN-1 (1 mm) for 1 h, and then loaded with FluoZin-3 for 30 min. In the presence of DPT (30 μM), the fluorescence observed at 60 min following SIN-1 exposure was reduced. A representative experiment of three that were performed is shown. (D) OLs in 96-well plates were treated with SIN-1 (1 mm) for 1 h, and then loaded with FluoZin-3 for 30 min. After washing, the fluorescence intensity (FI) of FluoZin-3 was immediately quantified and recorded using a fluorescence plate reader. *** $P<0.001$ was obtained when the SIN-1 treated groups were compared to the control groups in the absence and presence of DPT. The data shown are pooled from three different experiments.

(Fig. 6A). Consistently, we also found that SIN-1-induced ERK1/2 phosphorylation in cultures of OLs was attenuated by LPS pretreatment and the reduction was reversed when 1400W was co-applied (Fig. 6B). The effect of 1400W seems to be due to its reduction of iNOS expression (Fig. 6B) and the production of nitric oxide (Patel et al., 2004; He et al., 2010). The same results were also found when the LPS pretreated cultures were exposed to exogenous zinc (data not shown).

Mice with targeted genes deletion of gp91phox are resistant to EAE

Nitric oxide has long been suggested to be involved in the pathogenesis of MS (Bagasra et al., 1995; Hooper et al., 1997; Giovannoni et al., 1998; Brundin et al., 1999). However, it is still controversial whether nitric oxide is protective or detrimental to the disease (Brenner et al., 1997; Hooper et al., 1997; Fenyk-Melody et al., 1998; Sahrbacher et al., 1998; Dalton and Wittmer, 2005; Jack et al., 2007). The switch between the protective and the toxic effects of nitric oxide seems to be determined, at least in part, by the simultaneous generation of superoxide. NADPH oxidase is the primary source of superoxide in reactive microglia/macrophages. To determine the role of NADPH oxidase in the pathogenesis of MS, EAE was induced in mice with targeted gene deficiency of gp91phox, a catalytic component of the NADPH oxidase complex. As shown in Fig. 7, the clinical scores were significantly reduced in gp91phox−/− mice when compared to the wild type mice after EAE induction. Consistently, the typical loss of body weight observed in EAE wild type mice was prevented when EAE was induced in gp91phox−/− mice. At 28 days following EAE induction, the density of mature OLs labeled by CC1 in the spinal cord white matter was dramatically reduced in the wild type mice, but not in the knockout animals (Fig. 8A). Immunoreactivity to nitrotyrosine, indicative of peroxynitrite formation, was dramatically increased in the spinal cord white matter of the EAE wild type mice, which correlated with the loss of mature OLs (Fig. 8B). Nitrotyrosine immunoreactivity was not apparent in gp91phox−/− mice (Fig. 8B). Microglia reactivity observed in the EAE wild type mice was not present in the gp91phox−/− EAE mice (data not shown).

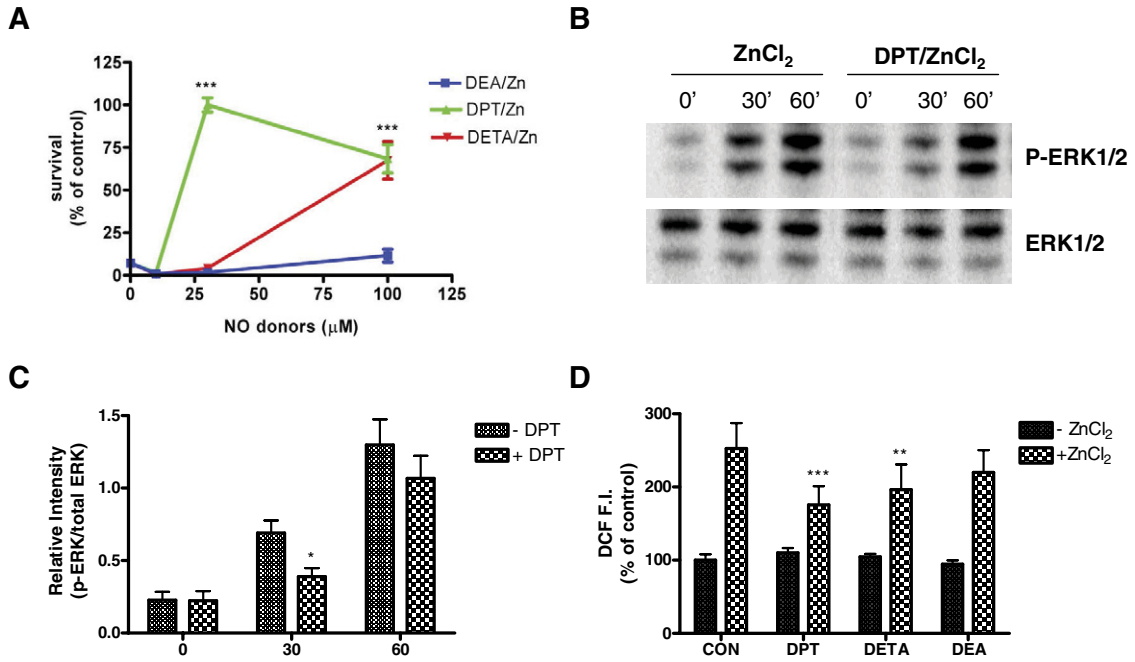

Fig. 5. Donors of nitric oxide attenuated zinc-induced toxicity, ERK phosphorylation and ROS accumulation. (A) Mature OLs were exposed to $ZnCl_2$ (300 μM) alone or with 30 μM and 100 μM DEA-NONOate (DEA), DPTA-NONOate (DPT), or DETA-NONOate (DETA) for 2 h, cell death was assessed at 24 h by assay of Alamar Blue reduction. $ZnCl_2$ at 300 μM caused complete OL death. DPT at 30 μM and 100 μM significantly blocked zinc induced toxicity to OLs. DETA at 100 μM was protective against zinc toxicity, but DEA was without effect. *** $P<0.001$ were obtained when the DPT- or the DETA- treated groups ($n=3$) were compared with the $ZnCl_2$ alone group ($n=3$). (B) Zinc caused a time-dependent increase of ERK phosphorylation. DPT attenuated ERK1/2 phosphorylation at 30 min following zinc treatment. A representative experiment of three that were performed is shown. (C) The relative intensity of the p-ERK/total ERK at various times following zinc treatment was measured using densitometry. * $P<0.05$ was obtained when the DPT plus zinc group was compared to the zinc alone group at 30 min following treatment. The data shown are pooled from three different experiments. (D) DPT and DETA, but not DEA attenuated zinc-induced ROS generation. OLs were exposed to $ZnCl_2$ (300 μM) for 90 min, and then the DCF fluorescence intensity (F.I.), an indicator of ROS generation, was quantitatively measured. ** $P<0.01$ and *** $P<0.001$ were obtained when the DPT- and DETA-treated groups ($n=3$) were compared with the $ZnCl_2$ alone group ($n=3$). For interpretation of the references to color in this figure legend, the reader is referred to the Web version of this article.

DISCUSSION

A growing body of evidence has shown that peroxynitrite, a reaction product between nitric oxide and superoxide near a diffusion-controlled rate, plays a pathogenic role in MS and the animal counterpart, EAE (Cross et al., 1997, 1998; Hooper et al., 1998, 2000; Scott et al., 2002; Bolton et al., 2008). Although the scavengers or the decomposition catalysts of peroxynitrite are consistently shown to ameliorate EAE (Cross et al., 2000; Hooper et al., 2000; Scott et al., 2002; Bolton et al., 2008), pharmacological inhibitors or genetic deletion of iNOS and NADPH oxidase, the primary enzymes for nitric oxide and superoxide production in reactive microglia or macrophages, often produce opposing results, with both beneficial and deleterious effects observed (Brenner et al., 1997; Hooper et al., 1997; Fenyk-Melody et al., 1998; Sahrbacher et al., 1998; van der Veen et al., 2000, 2004; Hultqvist et al., 2004). These results indicate that the interaction and the combined action between nitric oxide, superoxide and peroxynitrite are likely one of the potential determinants in the survival or death of OLs, the myelin producing cells in the CNS.

Nitric oxide is a weak oxidant, but the simultaneous generation of superoxide in close proximity to nitric oxide can result in the production of peroxynitrite, the most potent oxidant so far identified (Beckman et al., 1990; Beckman and Koppenol, 1996). Therefore, the outcome of the prooxidant versus the antioxidant properties of nitric oxide is highly dependent upon the production of superoxide. If the ratio of nitric oxide and superoxide is not favorable to the formation of peroxynitrite, increased production of nitric oxide may be protective, rather than destructive, when cells are exposed to the oxidative environments.

It has been reported that nitric oxide and peroxynitrite have contrasting effects toward axonal injury and demyelination in MS (van der Veen and Roberts, 1999; Touil et al., 2001). OLs are found to be resistant to nitric oxide, but more susceptible to the toxicity of peroxynitrite (Jack et al., 2007; Bishop et al., 2009). However, the mechanisms underlying the action of nitric oxide and peroxynitrite in OLs are unclear. In this study, we have found that ERK1/2 phosphorylation and 12-LOX activation, which are the critical components of peroxynitrite-mediated OL toxicity (Zhang et al., 2006), can be attenuated by exogenously, as well as endogenously generated nitric oxide. Interestingly, we found that 1400W, a selective iNOS inhibitor, also attenuated the expression of iNOS as reported by others (Patel et al., 2004; He et al., 2010). The mechanism for this inhibition is unclear. It is possible that the initial NO pro-

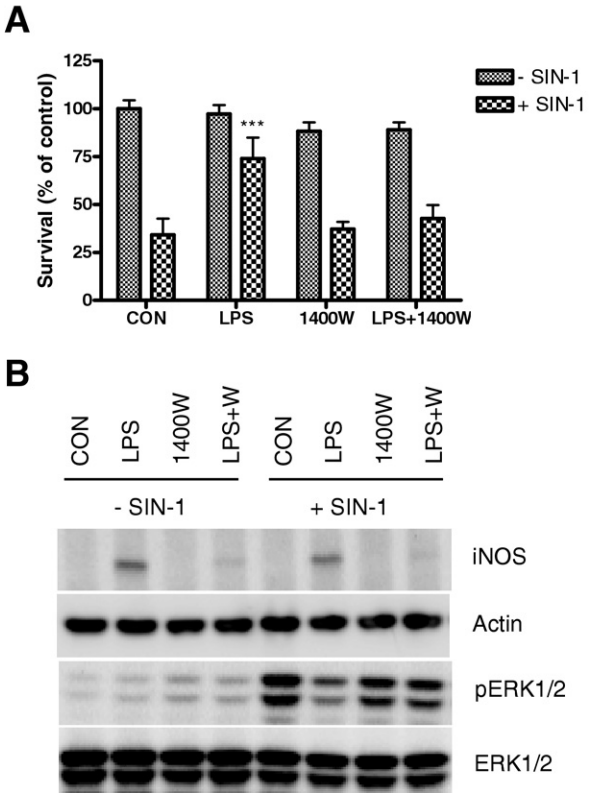

Fig. 6. LPS pretreatment enabled mature OL cultures resistant to SIN-1 induced toxicity and ERK1/2 phosphorylation. (A) Mature OL cultures were treated with LPS (5 μg/ml) for 24 h, and then treated with SIN-1 (0.5 mM) for 2 h. Toxicity was examined at 18–24 h. LPS preconditioning enabled mature OLs to be resistant to SIN-1 induced toxicity. The protection was eliminated when 1400W (10 μM) was used together with LPS. 1400W itself did not affect OL toxicity induced by SIN-1. *** $P<0.001$ was obtained when the LPS+SIN-1 group was compared with the other groups in the presence of SIN-1. The data shown are pooled from four different experiments. (B) LPS pretreatment enabled OLs resistant to SIN-1 induced ERK1/2 phosphorylation. OLs were pretreated with LPS, 1400W alone or in combination (LPS+W) for 24 h, followed by 1 h SIN-1 (1 mM) treatment. Cell lysates were used to detect the expression of iNOS, phosphorylated ERK1/2 (pERK1/2) and total ERK1/2. β-actin was used as a loading control. Treatment of cultures with LPS for 24 h induced iNOS expression and attenuated the ERK1/2 phosphorylation induced by SIN-1. The reduction of ERK1/2 phosphorylation was reversed when the selective iNOS inhibitor 1400W was co-administered with LPS. Notably, the expression of iNOS was also inhibited by 1400W. Pretreatment of cultures with 1400W had no effect on iNOS induction and ERK1/2 phosphorylation induced by SIN-1. LPS+W refer to LPS+1400W. A representative experiment of three that were performed is shown.

duction from iNOS may lead to the release of cytokines, which can further enhance the expression of iNOS. The use of 1400W may interrupt a cycle begetting further inflammation and iNOS expression (Patel et al., 2004). Consistent with the role of nitric oxide on cysteine depletion induced toxicity (Rosenberg et al., 1999), donors of nitric oxide with half lives of at least hours (such as DPTNONOate and DETA-NONOate), but not a few minutes (such as DEA-NONOate) protected against peroxynitrite or zinc induced toxicity. It is unlikely that a direct interaction between nitric oxide and peroxynitrite is attributable to the observed effect of nitric oxide on the basis of the following findings: (1) donors of nitric oxide did not affect SIN-1 evoked protein nitration in a cell-free system; (2) nitric oxide-induced cGMP accumulation was not affected by the presence of SIN-1; and (3) delayed addition of nitric oxide donors, which prevents the direct interaction between nitric oxide and peroxynitrite, also significantly attenuated peroxynitrite induced toxicity. These results suggest that the direct interaction of nitric oxide with the cell death signaling molecules, rather than with peroxynitrite itself, may contribute to the antioxidant effects of nitric oxide.

Nitric oxide is an important signaling molecule with diverse biological properties (Calabrese et al., 2007, 2009). Under physiological conditions, nitric oxide can react with iron (II) of the sGC, inducing a conformational change, and subsequently activating protein kinase G and protein phosphorylation (Garthwaite and Boulton, 1995).

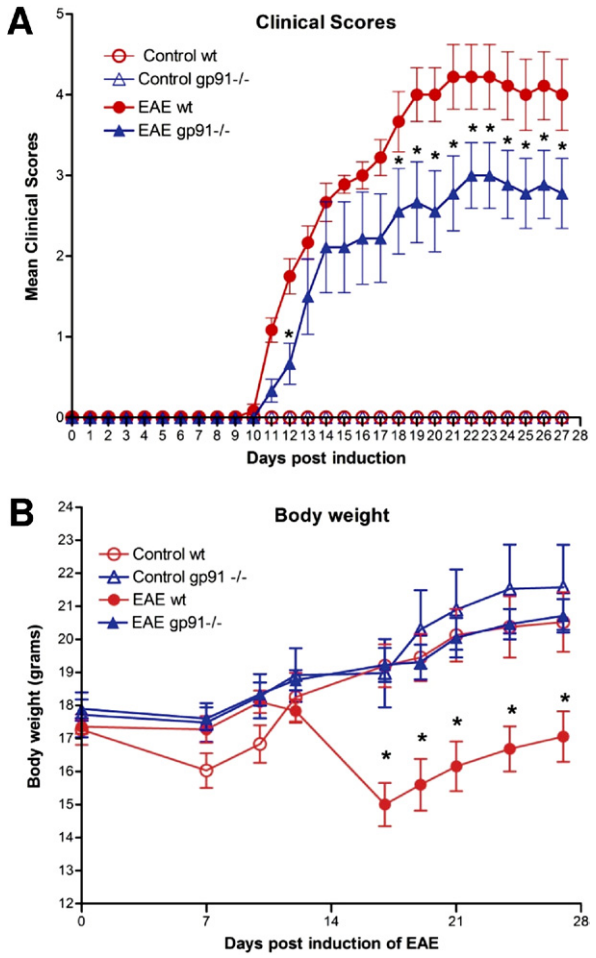

Fig. 7. Mice with targeted gene deletion of gp91phox are resistant to EAE. (A) gp91phox−/− mice and wild type C57BL/6J mice were inoculated with MOG35-55, and clinical scores were assessed on a daily basis. Clinical scores were significantly decreased in gp91phox−/− EAE mice ($n=8$) when compared to the EAE wild type mice ($n=8$; * $P<0.05$). (B) Body weight was significantly reduced in EAE wild type mice compared with EAE gp91phox−/−, wild type and gp91phox−/− control mice ($n=8$ in each group; * $P<0.05$). For interpretation of the references to color in this figure legend, the reader is referred to the Web version of this article.

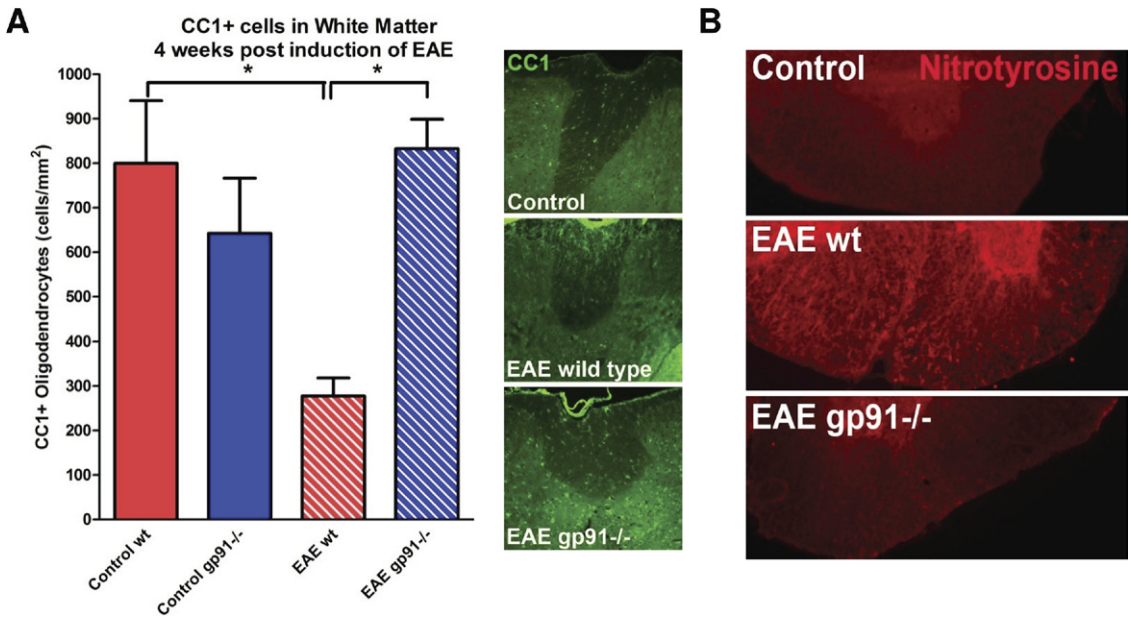

Fig. 8. Targeted gene deletion of gp91phox attenuated the loss of OLs and the formation of nitrotyrosine in the EAE mice spinal cord white matter. (A) A significant loss of CC1+ mature OLs was found in spinal cord white matter of EAE wild type mice, which was prevented in EAE gp91phox−/− mice ($n=8$; * $P<0.05$). A lower density of CC1 positive OL cells was readily observed in the dorsal column of EAE wild type mice compared with control and EAE gp91phox−/− mice. (B) Nitrotyrosine immunoreactivity, indicative of peroxynitrite formation, was reduced in the ventral white matter of EAE gp91phox−/− mice compared with the EAE wild type mice. A representative image from eight mice in each group is shown.

However, it seems unlikely that activation of sGC contributes to the protective effect of nitric oxide, because the protection of nitric oxide against SIN-1 toxicity is not affected by the presence of ^{1}H-[1,2,4] oxadiazolo[4,3-a] quinoxaline-1-one (ODQ), a selective inhibitor of sGC (data not shown). Nitric oxide can also mediate its biological effects via sGC independent pathways including protein nitrosation in many different cell types (Chung et al., 2005; Szabo et al., 2007; Calabrese et al., 2009). This posttranslational modification can either increase or decrease the protein function depending upon which protein is specifically targeted. It has been demonstrated that 5-LOX, the enzyme catalyzing the hydrolysis of arachidonic acid for the production of inflammatory leukotrienes, can be directly inhibited by nitric oxide (Coffey et al., 2000, 2002). Nitric oxide was also reported to directly inhibit the activity of 12-LOX (Nakatsuka and Osawa, 1994; Fujimoto et al., 1998; Coffey et al., 2001). The inhibitory action of nitric oxide to LOXs is suggested to be due to its reaction with the nonheme ions in the enzymes. It is also likely that nitrosation of the LOXs contribute to the inhibitory action of nitric oxide. Similar to the report that 5-LOX can be phosphorylated by MAPK-activated protein kinase (Werz et al., 2000), it is possible that 12-LOX can be directly, or indirectly, phosphorylated by ERK1/2 (Zhang et al., 2006). Therefore, the inhibitory action of nitric oxide on 12-LOX may be, at least partially, due to its attenuation of ERK phosphorylation.

We have previously shown that peroxynitrite toxicity to mature OLs is mediated by intracellular zinc release (Zhang et al., 2006). Although the exact sources of labile zinc is unclear, metallothioneins, the low molecular weight and cysteine-rich metal binding proteins, may be one of the major sources from which zinc is released typically in response to thiol oxidization (Maret, 2000). Similar to the redox agent 2,2′-dithiodipyridine (DTDP) (Aizenman et al., 2000), peroxynitrite can oxidize the cysteine residues of metallothioneins to readily release zinc ions (Zhang et al., 2006, 2007). Although many studies have suggested that nitric oxide can also liberate zinc from metallothioneins and the other intracellular zinc stores (St Croix et al., 2002; Spahl et al., 2003; Maret, 2006; Suh et al., 2008), we found the nitric oxide donor DPT-NONOate either used at 30 μM or 100 μM (data not shown) did not cause zinc release. DPT-NONOate had no effect on zinc liberation by peroxynitrite suggesting that nitric oxide can interact with the downstream signaling molecules activated by zinc. The partial inhibition of ERK and the complete blockage of 12-LOX activity by nitric oxide suggest that nitric oxide may block 12-LOX activity by its direct inhibition of the enzyme and its interference with the upstream pathways leading to 12-LOX activation. In addition, the antioxidant effect of nitric oxide may be also due to its direct reaction with alkoxyl and peroxyl intermediates during lipid peroxidation induced by peroxynitrite, thus terminating lipid radical chain propagated reactions (Rubbo et al., 1994, 2000; Baker et al., 2009).

EAE induced by myelin proteins is a commonly studied animal model of MS, which is characterized by T cell infiltration through a compromised blood–brain barrier. T cells interact with macrophage/microglia to affect disease progression by production of cytokines, chemokines, and nitric oxide. Although the initial response of reactive microglia/macrophages is phagocytosis of damaged cells or

tissues, increased production of the detrimental factors by microglia/macrophages can cause cytotoxicity. NADPH oxidase is believed to be the primary superoxide producing enzyme in reactive microglia and macrophages (Sun et al., 2007). It is a heterocomplex that is composed of p47phox, p67phox, gp91phox, p22phox, and rac2 (Rotrosen et al., 1993). Two of these subunits, p22phox and gp91phox are integral membrane proteins forming a heterodimeric flavocytochrome that is the catalytic core of the complex. The remaining components are cytosolic proteins. Upon activation, these cytosolic proteins translocate to the plasma membrane and form a functional heteromeric complex that associates with the membrane-bound heterodimer (Brown et al., 2003). Activated NADPH oxidase binds FAD and NADPH, resulting in a flow of electrons to oxygen to yield superoxide. Studies have shown that pharmacological inhibitors or targeted gene deletion of iNOS and gp91phox are protective against reactive microglia-induced toxicity to neurons and OLs in culture (Xie et al., 2002; Li et al., 2005). Although a number of studies have shown that deletion of iNOS potentiates the disease severity of EAE (Fenyk-Melody et al., 1998; Sahrbacher et al., 1998; van der Veen et al., 2000, 2004; Hultqvist et al., 2004; Farias et al., 2007), the contribution of NADPH oxidase in the pathogenesis of EAE has not been well elucidated. It has been reported that targeted gene deletion of p47phox can either increase or decrease the severity of several autoimmune diseases (van der Veen et al., 2000, 2004; Hultqvist et al., 2004). In this study, we found that EAE in gp91phox$-/-$ mice is ameliorated, supporting the notion that peroxynitrite plays a pathogenic role in EAE. It also suggests that without oxidation by superoxide, nitric oxide is likely to have immnosuppresive and anti-inflammatory effects (van der Veen et al., 2000). Our study also indicates that nitric oxide can attenuate peroxynitrite toxicity to OLs by directly targeting the cell death pathways involving ERK1/2 phosphorylation and 12-LOX activation. Taken together, these results suggest that blocking the formation specifically of peroxynitrite, rather than nitric oxide, may be a protective strategy against oxidative stress induced toxicity to OLs in diseases such as MS.

Acknowledgments—This work was supported by grants from the United Cerebral Palsy Foundation (R-759), the National Multiple Sclerosis Society (RG3741) and the start-up fund from the Uniformed Services University (R070 UX).

REFERENCES

Aizenman E, Stout AK, Hartnett KA, Dineley KE, McLaughlin B, Reynolds IJ (2000) Induction of neuronal apoptosis by thiol oxidation: putative role of intracellular zinc release. J Neurochem 75:1878–1888.

Babior BM, Lambeth JD, Nauseef W (2002) The neutrophil NADPH oxidase. Arch Biochem Biophys 397:342–344.

Back SA, Khan R, Gan X, Rosenberg PA, Volpe JJ (1999) A new Alamar Blue viability assay to rapidly quantify oligodendrocyte death. J Neurosci Methods 91:47–54.

Bagasra O, Michaels FH, Zheng YM, Bobroski LE, Spitsin SV, Fu ZF, Tawadros R, Koprowski H (1995) Activation of the inducible form of nitric oxide synthase in the brains of patients with multiple sclerosis. Proc Natl Acad Sci U S A 92:12041–12045.

Baker PR, Schopfer FJ, O'Donnell VB, Freeman BA (2009) Convergence of nitric oxide and lipid signaling: anti-inflammatory nitrofatty acids. Free Radic Biol Med 46:989–1003.

Baud O, Li J, Zhang Y, Neve RL, Volpe JJ, Rosenberg PA (2004) Nitric oxide-induced cell death in developing oligodendrocytes is associated with mitochondrial dysfunction and apoptosis-inducing factor translocation. Eur J Neurosci 20:1713–1726.

Beckman JS, Beckman TW, Chen J, Marshall PA, Freeman BA (1990) Apparent hydroxyl radical production by peroxynitrite: implications for endothelial injury from nitric oxide and superoxide. Proc Natl Acad Sci U S A 87:1620–1624.

Beckman JS, Koppenol WH (1996) Nitric oxide, superoxide, and peroxynitrite: the good, the bad, and ugly. Am J Physiol 271: C1424–C1437.

Bishop A, Hobbs KG, Eguchi A, Jeffrey S, Smallwood L, Pennie C, Anderson J, Estevez AG (2009) Differential sensitivity of oligodendrocytes and motor neurons to reactive nitrogen species: implications for multiple sclerosis. J Neurochem 109:93–104.

Bolton C, Scott GS, Smith T, Flower RJ (2008) The acute and chronic phases of chronic relapsing experimental autoimmune encephalomyelitis (CR EAE) are ameliorated by the peroxynitrite decomposition catalyst, 5,10,15,20-tetrakis(4-sulfonatophenyl)porphyrinatoiron (III) chloride, (FeTPPS). Eur J Pharmacol 601:88–93.

Brenner T, Brocke S, Szafer F, Sobel RA, Parkinson JF, Perez DH, Steinman L (1997) Inhibition of nitric oxide synthase for treatment of experimental autoimmune encephalomyelitis. J Immunol 158: 2940–2946.

Broholm H, Andersen B, Wanscher B, Frederiksen JL, Rubin I, Pakkenberg B, Larsson HB, Lauritzen M (2004) Nitric oxide synthase expression and enzymatic activity in multiple sclerosis. Acta Neurol Scand 109:261–269.

Brown GE, Stewart MQ, Liu H, Ha VL, Yaffe MB (2003) A novel assay system implicates PtdIns(3,4)P(2), PtdIns(3)P, and PKC delta in intracellular production of reactive oxygen species by the NADPH oxidase. Mol Cell 11:35–47.

Brundin L, Morcos E, Olsson T, Wiklund NP, Andersson M (1999) Increased intrathecal nitric oxide formation in multiple sclerosis; cerebrospinal fluid nitrite as activity marker. Eur J Neurol 6: 585–590.

Calabrese V, Cornelius C, Rizzarelli E, Owen JB, Dinkova-Kostova AT, Butterfield DA (2009) Nitric oxide in cell survival: a janus molecule. Antioxid Redox Signal 11:2717–2739.

Calabrese V, Mancuso C, Calvani M, Rizzarelli E, Butterfield DA, Stella AM (2007) Nitric oxide in the central nervous system: neuroprotection versus neurotoxicity. Nat Rev Neurosci 8:766–775.

Chung KK, Dawson TM, Dawson VL (2005) Nitric oxide, S-nitrosylation and neurodegeneration. Cell Mol Biol Noisy-le-grand 51:247–254.

Coffey MJ, Natarajan R, Chumley PH, Coles B, Thimmalapura PR, Nowell M, Kuhn H, Lewis MJ, Freeman BA, O'Donnell VB (2001) Catalytic consumption of nitric oxide by 12/15- lipoxygenase: inhibition of monocyte soluble guanylate cyclase activation. Proc Natl Acad Sci U S A 98:8006–8011.

Coffey MJ, Phare SM, Peters-Golden M (2000) Prolonged exposure to lipopolysaccharide inhibits macrophage 5-lipoxygenase metabolism via induction of nitric oxide synthesis. J Immunol 165: 3592–3598.

Coffey MJ, Phare SM, Peters-Golden M (2002) Interaction between nitric oxide, reactive oxygen intermediates, and peroxynitrite in the regulation of 5-lipoxygenase metabolism. Biochim Biophys Acta 1584:81–90.

Cross AH, Manning PT, Keeling RM, Schmidt RE, Misko TP (1998) Peroxynitrite formation within the central nervous system in active multiple sclerosis. J Neuroimmunol 88:45–56.

Cross AH, Manning PT, Stern MK, Misko TP (1997) Evidence for the production of peroxynitrite in inflammatory CNS demyelination. J Neuroimmunol 80:121–130.

Cross AH, San M, Stern MK, Keeling RM, Salvemini D, Misko TP (2000) A catalyst of peroxynitrite decomposition inhibits murine experimental autoimmune encephalomyelitis. J Neuroimmunol 107:21–28.

Dalton DK, Wittmer S (2005) Nitric-oxide-dependent and independent mechanisms of protection from CNS inflammation during Th1-mediated autoimmunity: evidence from EAE in iNOS KO mice. J Neuroimmunol 160:110–121.

Encinas JM, Manganas L, Enikolopov G (2005) Nitric oxide and multiple sclerosis. Curr Neurol Neurosci Rep 5:232–238.

Farias AS, de la Hoz C, Castro FR, Oliveira EC, Ribeiro dos Reis JR, Silva JS, Langone F, Santos LM (2007) Nitric oxide and TNFalpha effects in experimental autoimmune encephalomyelitis demyelination. Neuroimmunomodulation 14:32–38.

Fenyk-Melody JE, Garrison AE, Brunnert SR, Weidner JR, Shen F, Shelton BA, Mudgett JS (1998) Experimental autoimmune encephalomyelitis is exacerbated in mice lacking the NOS2 gene. J Immunol 160:2940–2946.

Fujimoto Y, Tagano S, Ogawa K, Sakuma S, Fujita T (1998) Comparison of the effects of nitric oxide and peroxynitrite on the 12-lipoxygenase and cyclooxygenase metabolism of arachidonic acid in rabbit platelets. Prostaglandins Leukot Essent Fatty Acids 59:95–100.

Garthwaite J, Boulton CL (1995) Nitric oxide signaling in the central nervous system. Annu Rev Physiol 57:683–706.

Gee KR, Zhou ZL, Qian WJ, Kennedy R (2002) Detection and imaging of zinc secretion from pancreatic beta-cells using a new fluorescent zinc indicator. J Am Chem Soc 124:776–778.

Giovannoni G, Heales SJ, Land JM, Thompson EJ (1998) The potential role of nitric oxide in multiple sclerosis. Mult Scler 4:212–216.

He YF, Chen HJ, Qian LH, Chen GY (2010) Effect of 1400W on blocking lipopolysaccharide-induced microglial toxicity to preoligodendrocytes. World J Pediatr 6:249–254.

Hewett JA, Hewett SJ, Winkler S, Pfeiffer SE (1999) Inducible nitric oxide synthase expression in cultures enriched for mature oligodendrocytes is due to microglia. J Neurosci Res 56:189–198.

Hill KE, Zollinger LV, Watt HE, Carlson NG, Rose JW (2004) Inducible nitric oxide synthase in chronic active multiple sclerosis plaques: distribution, cellular expression and association with myelin damage. J Neuroimmunol 151:171–179.

Hooper DC, Bagasra O, Marini JC, Zborek A, Ohnishi ST, Kean R, Champion JM, Sarker AB, Bobroski L, Farber JL, Akaike T, Maeda H, Koprowski H (1997) Prevention of experimental allergic encephalomyelitis by targeting nitric oxide and peroxynitrite: implications for the treatment of multiple sclerosis. Proc Natl Acad Sci U S A 94:2528–2533.

Hooper DC, Scott GS, Zborek A, Mikheeva T, Kean RB, Koprowski H, Spitsin SV (2000) Uric acid, a peroxynitrite scavenger, inhibits CNS inflammation, blood-CNS barrier permeability changes, and tissue damage in a mouse model of multiple sclerosis. FASEB J 14:691–698.

Hooper DC, Spitsin S, Kean RB, Champion JM, Dickson GM, Chaudhry I, Koprowski H (1998) Uric acid, a natural scavenger of peroxynitrite, in experimental allergic encephalomyelitis and multiple sclerosis. Proc Natl Acad Sci U S A 95:675–680.

Hultqvist M, Olofsson P, Holmberg J, Backstrom BT, Tordsson J, Holmdahl R (2004) Enhanced autoimmunity, arthritis, and encephalomyelitis in mice with a reduced oxidative burst due to a mutation in the Ncf1 gene. Proc Natl Acad Sci U S A 101:12646–12651.

Jack C, Antel J, Bruck W, Kuhlmann T (2007) Contrasting potential of nitric oxide and peroxynitrite to mediate oligodendrocyte injury in multiple sclerosis. Glia 55:926–934.

Knowles RG, Moncada S (1994) Nitric oxide synthases in mammals. Biochem J 298 (Pt 2):249–258.

Li J, Baud O, Vartanian T, Volpe JJ, Rosenberg PA (2005) Peroxynitrite generated by inducible nitric oxide synthase and NADPH oxidase mediates microglial toxicity to oligodendrocytes. Proc Natl Acad Sci U S A 102:9936–9941.

Maragos CM, Morley D, Wink DA, Dunams TM, Saavedra JE, Hoffman A, Bove AA, Isaac L, Hrabie JA, Keefer LK (1991) Complexes of NO with nucleophiles as agents for the controlled biological release of nitric oxide. Vasorelaxant effects. J Med Chem 34: 3242–3247.

Maret W (2000) The function of zinc metallothionein: a link between cellular zinc and redox state. J Nutr 130:1455S–1458S.

Maret W (2006) Zinc coordination environments in proteins as redox sensors and signal transducers. Antioxid Redox Signal 8:1419–1441.

Misko TP, Highkin MK, Veenhuizen AW, Manning PT, Stern MK, Currie MG, Salvemini D (1998) Characterization of the cytoprotective action of peroxynitrite decomposition catalysts. J Biol Chem 273:15646–15653.

Mooradian DL, Hutsell TC, Keefer LK (1995) Nitric oxide (NO) donor molecules: effect of NO release rate on vascular smooth muscle cell proliferation *in vitro*. J Cardiovasc Pharmacol 25:674–678.

Murad F, Forstermann U, Nakane M, Pollock J, Tracey R, Matsumoto T, Buechler W (1993) The nitric oxide-cyclic GMP signal transduction system for intracellular and intercellular communication. Adv Second Messenger Phosphoprotein Res 28:101–109.

Nakatsuka M, Osawa Y (1994) Selective inhibition of the 12-lipoxygenase pathway of arachidonic acid metabolism by L-arginine or sodium nitroprusside in intact human platelets. Biochem Biophys Res Commun 200:1630–1634.

Pacher P, Beckman JS, Liaudet L (2007) Nitric oxide and peroxynitrite in health and disease. Physiol Rev 87:315–424.

Patel P, Qi WN, Allen DM, Chen LE, Seaber AV, Stamler JS, Urbaniak JR (2004) Inhibition of iNOS with 1400W improves contractile function and alters nos gene and protein expression in reperfused skeletal muscle. Microsurgery 24:324–331.

Robinson KM, Morre JT, Beckman JS (2004) Triuret: a novel product of peroxynitrite-mediated oxidation of urate. Arch Biochem Biophys 423:213–217.

Rosenberg PA, Li Y, Ali S, Altiok N, Back SA, Volpe JJ (1999) Intracellular redox state determines whether nitric oxide is toxic or protective to rat oligodendrocytes in culture. J Neurochem 73: 476–484.

Rotrosen D, Yeung CL, Katkin JP (1993) Production of recombinant cytochrome b558 allows reconstitution of the phagocyte NADPH oxidase solely from recombinant proteins. J Biol Chem 268: 14256–14260.

Rubbo H, Radi R, Anselmi D, Kirk M, Barnes S, Butler J, Eiserich JP, Freeman BA (2000) Nitric oxide reaction with lipid peroxyl radicals spares alpha-tocopherol during lipid peroxidation. Greater oxidant protection from the pair nitric oxide/alpha-tocopherol than alpha-tocopherol/ascorbate. J Biol Chem 275:10812–10818.

Rubbo H, Radi R, Trujillo M, Telleri R, Kalyanaraman B, Barnes S, Kirk M, Freeman BA (1994) Nitric oxide regulation of superoxide and peroxynitrite-dependent lipid peroxidation. Formation of novel nitrogen-containing oxidized lipid derivatives. J Biol Chem 269: 26066–26075.

Saha RN, Pahan K (2006) Regulation of inducible nitric oxide synthase gene in glial cells. Antioxid Redox Signal 8:929–947.

Sahrbacher UC, Lechner F, Eugster HP, Frei K, Lassmann H, Fontana A (1998) Mice with an inactivation of the inducible nitric oxide synthase gene are susceptible to experimental autoimmune encephalomyelitis. Eur J Immunol 28:1332–1338.

Scott GS, Spitsin SV, Kean RB, Mikheeva T, Koprowski H, Hooper DC (2002) Therapeutic intervention in experimental allergic encephalomyelitis by administration of uric acid precursors. Proc Natl Acad Sci U S A 99:16303–16308.

Sensi SL, Ton-That D, Weiss JH, Rothe A, Gee KR (2003) A new mitochondrial fluorescent zinc sensor. Cell Calcium 34:281–284.

Shornick LP, Holtzman MJ (1993) A cryptic, microsomal-type arachidonate 12-lipoxygenase is tonically inactivated by oxidation-reduction conditions in cultured epithelial cells. J Biol Chem 268: 371–376.

Smith KJ, Lassmann H (2002) The role of nitric oxide in multiple sclerosis. Lancet Neurol 1:232–241.

Spahl DU, Berendji-Grun D, Suschek CV, Kolb-Bachofen V, Kroncke KD (2003) Regulation of zinc homeostasis by inducible NO synthase-derived NO: nuclear metallothionein translocation and intranuclear Zn^{2+} release. Proc Natl Acad Sci U S A 100: 13952–13957.

Spitsin S, Hooper DC, Leist T, Streletz LJ, Mikheeva T, Koprowskil H (2001) Inactivation of peroxynitrite in multiple sclerosis patients after oral administration of inosine may suggest possible approaches to therapy of the disease. Mult Scler 7:313–319.

St Croix CM, Wasserloos KJ, Dineley KE, Reynolds IJ, Levitan ES, Pitt BR (2002) Nitric oxide-induced changes in intracellular zinc homeostasis are mediated by metallothionein/thionein. Am J Physiol Lung Cell Mol Physiol 282:L185–L192.

Suh SW, Hamby AM, Gum ET, Shin BS, Won SJ, Sheline CT, Chan PH, Swanson RA (2008) Sequential release of nitric oxide, zinc, and superoxide in hypoglycemic neuronal death. J Cereb Blood Flow Metab 28:1697–1706.

Sun GY, Horrocks LA, Farooqui AA (2007) The roles of NADPH oxidase and phospholipases A2 in oxidative and inflammatory responses in neurodegenerative diseases. J Neurochem 103: 1–16.

Sun J, Druhan LJ, Zweier JL (2010) Reactive oxygen and nitrogen species regulate inducible nitric oxide synthase function shifting the balance of nitric oxide and superoxide production. Arch Biochem Biophys 494:130–137.

Szabo C, Ischiropoulos H, Radi R (2007) Peroxynitrite: biochemistry, pathophysiology and development of therapeutics. Nat Rev Drug Discov 6:662–680.

Thomas DD, Ridnour LA, Isenberg JS, Flores-Santana W, Switzer CH, Donzelli S, Hussain P, Vecoli C, Paolocci N, Ambs S, Colton CA, Harris CC, Roberts DD, Wink DA (2008) The chemical biology of nitric oxide: implications in cellular signaling. Free Radic Biol Med 45:18–31.

Touil T, Deloire-Grassin MS, Vital C, Petry KG, Brochet B (2001) *In vivo* damage of CNS myelin and axons induced by peroxynitrite. Neuroreport 12:3637–3644.

van der Veen RC, Dietlin TA, Hofman FM, Pen L, Segal BH, Holland SM (2000) Superoxide prevents nitric oxide-mediated suppression of helper T lymphocytes: decreased autoimmune encephalomyelitis in nicotinamide adenine dinucleotide phosphate oxidase knockout mice. J Immunol 164:5177–5183.

van der Veen RC, Dietlin TA, Karapetian A, Holland SM, Hofman FM (2004) Extra-cellular superoxide promotes T cell expansion through inactivation of nitric oxide. J Neuroimmunol 153:183–189.

van der Veen RC, Roberts LJ (1999) Contrasting roles for nitric oxide and peroxynitrite in the peroxidation of myelin lipids. J Neuroimmunol 95:1–7.

Wang H, Li J, Follett PL, Zhang Y, Cotanche DA, Jensen FE, Volpe JJ, Rosenberg PA (2004) 12-Lipoxygenase plays a key role in cell death caused by glutathione depletion and arachidonic acid in rat oligodendrocytes. Eur J Neurosci 20:2049–2058.

Werz O, Klemm J, Samuelsson B, Radmark O (2000) 5-Lipoxygenase is phosphorylated by p38 kinase-dependent MAPKAP kinases. Proc Natl Acad Sci U S A 97:5261–5266.

Willenborg DO, Staykova M, Fordham S, O'Brien N, Linares D (2007) The contribution of nitric oxide and interferon gamma to the regulation of the neuro-inflammation in experimental autoimmune encephalomyelitis. J Neuroimmunol 191:16–25.

Wu M, Tsirka SE (2009) Endothelial NOS-deficient mice reveal dual roles for nitric oxide during experimental autoimmune encephalomyelitis. Glia 57:1204–1215.

Xie Z, Wei M, Morgan TE, Fabrizio P, Han D, Finch CE, Longo VD (2002) Peroxynitrite mediates neurotoxicity of amyloid beta-peptide1-42- and lipopolysaccharide-activated microglia. J Neurosci 22:3484–3492.

Yao S, Pandey P, Ljunggren-Rose A, Sriram S (2010) LPS mediated injury to oligodendrocytes is mediated by the activation of nNOS: relevance to human demyelinating disease. Nitric Oxide 22: 197–204.

Zhang Y, Aizenman E, DeFranco DB, Rosenberg PA (2007) Intracellular zinc release, 12-lipoxygenase activation and MAPK dependent neuronal and oligodendroglial death. Mol Med 13:350–355.

Zhang Y, Rosenberg PA (2002) The essential nutrient pyrroloquinoline quinone may act as a neuroprotectant by suppressing peroxynitrite formation. Eur J Neurosci 16:1015–1024.

Zhang Y, Wang H, Li J, Dong L, Xu P, Chen W, Neve RL, Volpe JJ, Rosenberg PA (2006) Intracellular zinc release and ERK phosphorylation are required upstream of 12-lipoxygenase activation in peroxynitrite toxicity to mature rat oligodendrocytes. J Biol Chem 281:9460–9470.

Zhang Y, Wang H, Li J, Jimenez DA, Levitan ES, Aizenman E, Rosenberg PA (2004) Peroxynitrite-induced neuronal apoptosis is mediated by intracellular zinc release and 12-lipoxygenase activation. J Neurosci 24:10616–10627.

(Accepted 5 April 2011)
(Available online 13 April 2011)